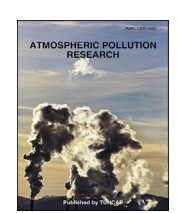
HOSTED BY

Contents lists available at ScienceDirect

Atmospheric Pollution Research

journal homepage: http://www.journals.elsevier.com/locate/apr



Original article

Characteristics and sources of PM in seasonal perspective — A case study from one year continuously sampling in Beijing



Rongrong Shen ^{a, *}, Klaus Schäfer ^a, Jürgen Schnelle-Kreis ^b, Longyi Shao ^c, Stefan Norra ^{d, e, f}, Utz Kramar ^e, Bernhard Michalke ^g, Gülcin Abbaszade ^b, Thorsten Streibel ^h, Mathieu Fricker ⁱ, Yuan Chen ^e, Ralf Zimmermann ^{b, h}, Stefan Emeis ^a, Hans Peter Schmid ^a

- ^a Institute of Meteorology and Climate Research, Atmospheric Environmental Research, Karlsruhe Institute of Technology (KIT/IMK-IFU), 82467 Garmisch-Partenkirchen, Germany
- b Joint Mass Spectrometry Centre, Comprehensive Molecular Analytics, Helmholtz Zentrum München (HMGU/CMA), 85764 Neuherberg, Germany
- ^c School of Geoscience and Surveying Engineering, China University of Mining and Technology (Beijing) (CUMTB), 100083 Beijing, PR China
- ^d Institute of Geography and Geoecology, Karlsruhe Institute of Technology (KIT/IGG), 76128 Karlsruhe, Germany
- ^e Institute of Mineralogy and Geochemistry, Karlsruhe Institute of Technology (KIT/IMG), 76128 Karlsruhe, Germany
- f Institute of Mineralogy, TU Bergakademie Freiberg (TUBF), 09596 Freiberg, Germany
- g Research Unit Analytical BioGeoChemistry, Helmholtz Zentrum München (HMGU/ABGC), 85764 Neuherberg, Germany
- ^h Joint Mass Spectrometry Centre, Chair of Analytical Chemistry, University of Rostock (UR/IC), 18059 Rostock, Germany
- ⁱ Research Center Human Biometeorology, Air Quality Department, Deutscher Wetterdienst (DWD/AQD), 79104 Freiburg, Germany

ARTICLE INFO

Article history:
Received 14 June 2015
Received in revised form
7 September 2015
Accepted 7 September 2015
Available online 21 October 2015

Keywords:
Seasonal variation
Characteristics
Source apportionment
PMF
Back trajectory cluster analyses

ABSTRACT

Daily mass concentrations and chemical compositions (elemental carbon, organic carbon, water soluble ions, chemical elements and organic species) of PM were measured continuously in Beijing for one year from June 2010 to June 2011 (365 samples). The seasonal variation of PM mass concentration followed the order of spring 2011 > winter 2010 > summer 2010 > autumn 2010. Organic matter (OM) and secondary inorganic aerosol components (SNA: SO_4^2 , NO_3 and NH_4^+) were the two major fractions of PM during the whole year. Source apportionment by PMF performed on the basis of a full year of data, including both inorganic and organic species, showed that biomass burning, secondary sulfate and nitrate formation, mineral dust, industry, coal combustion and traffic were the main sources of PM in Beijing during 2010-2011. Specifically, comparison among the four seasons shows that the contribution of secondary sulfate and biomass burning, secondary nitrate formation, mineral dust, and coal combustion were the dominating sources of PM in summer, autumn, spring and winter, respectively. The contributions of industry to PM was distributed evenly in four seasons, while traffic contributed more in summer and autumn than in winter and spring. Backward trajectory analysis was applied in combination with PMF and showed that air flow from the South contributed mostly to high PM mass concentrations in Beijing, Meteorological parameters (temperature, wind speed, wind direction, precipitation and mixing layer height) influence such a variation. In general, high relative humidity and low mixing layer height can raise PM mass concentration, while high wind speed and precipitation can reduce pollutants. In addition, wind direction also plays a key role in influencing PM because different wind directions can bring different pollutants to Beijing from different regions.

Copyright © 2015 Turkish National Committee for Air Pollution Research and Control. Production and hosting by Elsevier B.V. All rights reserved.

* Corresponding author. Tel.: +49 8821 183192; fax: +49 8821 73573. E-mail address: Rongrong_Shen@sina.com (R. Shen).

Peer review under responsibility of Turkish National Committee for Air Pollution Research and Control.

1. Introduction

PM, as the major air pollutant in Beijing, has been widely studied on the general chemical characteristics (Song et al., 2012; Zhao et al., 2013a) and certain specific species, such as carbonaceous components (Yang et al., 2011; Zhao et al., 2013b), inorganic elements (Shi

et al., 2005; Yang et al., 2012), inorganic ions (Yao et al., 2002; Ianniello et al., 2011), organic matter (Sun et al., 2012; Wang et al., 2012) as well as on health effects (Shao et al., 2006, 2007; Li et al., 2010; Dimitrova et al., 2012), and influence on visibility (Jung and Kim, 2006; Cao et al., 2012) and global climate (IPCC, 2013).

In order to improve air quality, source apportionment of PM in Beijing was also widely performed by different receptor models, such as chemical mass balance (CMB), positive matrix factorization (PMF) and principal component analysis (PCA). However, in the receptor models mentioned above, PMF is discussed to be the most suitable tool for source apportionment. The reason is that PMF does not need a priori information on source emission profiles when compared with CMB, and PMF can constrain the factors and their loadings to be non-negative in value and handle missing data (Paatero and Tapper, 1994; Paatero, 1997) when compared with PCA. Even though lots of studies on source apportionment of PM in Beijing have been done by PMF (Lei et al., 2004; Song et al., 2006, 2007; Zhang et al., 2007; Wang et al., 2008, 2009; Yu et al., 2013; Wu et al., 2014), these studies only used either inorganic or organic compounds to perform source apportionment and the durations of sampling were comparably short or discontinuous. Sources and characteristics of PM samples from a short or discontinuous sampling period cannot be satisfactorily representative of the whole year. A previous study (Zhang et al., 2009a) pointed out that not less than 90 samples should be analyzed to obtain robust PMF results when 48 chemical species were included in the analysis. Of course more observations increase the robustness of source contribution analysis.

Consequently, a full year of continuous data was investigated to obtain more robust source apportionment and to investigate the temporal variation of source contributions. Source apportionment of PM in Beijing with continuous long-term inorganic and organic compounds has not previously been reported. Here, for the first time, data from a sampling campaign covering a full year of PM sampling are investigated. Both inorganic and organic composition was analyzed in this study and source apportionment based on a full year of continuous data was conducted.

Daily PM samples were collected continuously for one year from June 2010 until June 2011. Elemental carbon (EC), organic carbon (OC), inorganic elements, water soluble ions, PAHs, hopanes and levoglucosan were quantified. Source apportionment of PM was performed by PMF on the basis of these chemical compounds. The objectives of this paper are: (1) to investigate PM level at the height for exposure to humans; (2) to study the annual and seasonal variation of inorganic and organic species mass concentrations; (3) to obtain the more robust source apportionment results based on a large data set; (4) to look into the seasonal variation of different sources contribution to PM; (5) to examine the contribution of different sources in different air flows; (6) to discuss typical PM chemical characteristics during the four seasons together with meteorological influences.

2. Materials and methods

2.1. Sampling methods

Two sequential High-Volume Samplers (HVS, nominal flow 500 l min⁻¹, Digitel DHA-80, Hegnau, Switzerland), sampler A and sampler B, were installed at the campus of the China University of Geosciences (Beijing) (CUGB) (Fig. 1). PM samples (00:00–24:00) were collected in parallel from 21 June 2010 till 20 June 2011. Quartz fiber filters (Munktell T293, Falun, Sweden) with 150 mm diameter were used as the collection substrate. One field blank sample from both samplers was collected every second week. The sampler inlet tubes were installed at a height of 2 m above ground, which is a typical height for the exposure of humans.

2.2. Analytical methods

Filters of sampler A were heated at 500 °C for 6 h before sampling and analyzed for EC, OC, water soluble ions and organic compounds. Filters of sampler B were weighed by an analytical balance (Mettler Analysenwaage AE240, reading precision 0.1 mg) before and after sampling for gravimetric PM mass concentration determination. A 48 h equilibration of filters at a temperature of 22 °C \pm 0.2 °C and a relative humidity (RH) of 42% \pm 0.5% in a conditioning room was conducted before weighing. Filters of sampler B were also used for inorganic elements analysis.

OC and EC were analyzed by a thermal/optical carbon analyser (DRI Model 2001A, Desert Research Institute, USA). The IMPROVE (Interagency Monitoring of Protected Visual Environments) A protocol and the thermal optical reflection method (TOR) are applied. Round filter parts with 8 mm diameter were punched from each loaded sample and heated gradually at different temperatures for measuring different OC (OC1, OC2, OC3 and OC4) and EC fractions (EC1, EC2 and EC3). OC and EC have been corrected by the value of optical pyrolyzed carbon (OPC) (OC=OC1+OC2+OC3+OC4+OPC; EC = EC1+EC2+EC3-OPC). More details of this method can be found in previous studies (Chow et al., 2007; Li et al., 2012a).

Inorganic elements, including K, Ca, Ti, Cr, Mn, Fe, Ni, Cu, Zn, As, Sn, Sb, Ba and Pb, were measured by polarized energy dispersive X-ray fluorescence (PEDXRF, Epsilon 5, PANalytical, The Netherlands). All loaded filters were analyzed as thin layer samples, using for calibration 30 filters of different load, which were previously analyzed by Inductively coupled plasma mass spectrometry (ICP-MS). More details of this method are described by Kramar (1999).

Cl $^-$, NO $_3^-$ and SO $_4^{2-}$ were analyzed by ion chromatography (IC) (ICS-1500, Dionex, USA) and NH $_4^+$ by a continuous flow analyser (CFA) (Scan $^{++}$, Skalar, The Netherlands). Round filter parts with 25 mm diameter were punched from loaded filters and extracted by 5 ml de-ionized water (Milli-Q, 18.2 M Ω cm) in an ultrasonic bath for 15 min. The extraction was taken for three times and the solution was filtered by 0.45 μ m syringe filter after each extraction. 15 ml extracted solution was obtained for each sample in total

Levoglucosan, eleven Hopane substances and fifteen PAHs were measured by in-situ derivatisation direct thermal desorption gas chromatography time-of-flight mass spectrometry (IDTD-GC-TOFMS). An Agilent 6890 gas chromatograph (Agilent, USA) attached to a Pegasus III time of flight mass spectrometer (Leco, USA) was used. The eleven Hopane substances are 18α(H)-22,29,30-Trisnorneohopane (Ts), $17\alpha(H)$ -22,29,30-Trisnorhopane (Tm), $17\beta(H)-22,29,30$ -Trisnorhopane (27b), $17\alpha(H)21\beta(H)-30$ -Norhopane (29ab), $17\beta(H)21\alpha(H)-30$ -Norhopane (29ba), $17\alpha(H)$ $21\beta(H)$ -Hopane (30ab), $17\beta(H)21\alpha(H)$ -Hopane (Moretan) (30ba), 22S-17α(H)21β(H)-Homohopane (31abS), 22R-17α(H)21β(H)-Homohopane (31abR), 22S-17 α (H)21 β (H)-Bishomohopane (32abS), and $22R-17\alpha(H)21\beta(H)$ -Bishomohopane (32abR). The fifteen PAHs are Phenanthrene (PHE), Anthracene (ANT), Pyrene (PYR), Fluoranthene (FLU), Benz[a]anthracene (BAA), Chrysene (CRY), sum of Benzfluoranthenes (BBKF), Benzo[e]pyrene (BEP), Benzo[a]pyrene (BAP), Perylene (PER), Dibenz[a,h]anthracene (DAH), Indeno[1,2,3cd|pyrene (IND), Picene (PIC), Benzo[ghi])perylene (BGH), and Coronene (COR). However, PHE, ANT, PYR and FLU are considered to be semi-volatile and thus mainly present in the gas phase. As the mass concentrations of these compounds determined in PM samples are highly driven by the gas phase concentrations during the last minutes of sampling, PHE, ANT, PYR and FLU are excluded from discussion in this study. More details of this method are described by Orasche et al. (2011).



Fig. 1. The location of the sampling sites in Beijing (Source: http://map.baidu.com): CUGB is the China University of Geosciences (Beijing); IAP is the Institute of Atmospheric Physics of the Chinese Academy of Sciences; ZBAA is the code for the monitoring site from where one can obtain meteorological data on the website of the University of Wyoming, USA (http://weather.uwyo.edu/upperair/sounding.html).

2.3. Meteorological parameters

Meteorological data, including temperature (T), atmospheric pressure (p), relative humidity (RH), visibility, wind speed (WS) and wind direction (WD), were collected from the internet page of the University of Wyoming, USA (http://weather.uwyo.edu/upperair/sounding.html) where the data of the weather station ZBAA (Fig. 1) is available. The available maximum visibility data is only up to 10 km. Wind roses were produced from ZBAA half hourly wind data with WRPLOT View Freeware (Lakes Environmental, Ontario, Canada).

Mixing layer height (MLH) was determined by a ceilometer CL31 (Vaisala GmbH, Hamburg, Germany), a laser-based remote sensing system (mini lidar), at the IAP (Institute of Atmospheric Physics) (Fig. 1). All details about methods of MLH calculation from particle backscatter intensities are described in previous studies (Münkel et al., 2007; Emeis et al., 2008).

2.4. Positive matrix factorization (PMF)

PMF is one kind of multivariate factor analysis methods which uses a matrix of measured data and a matrix of known uncertainties of individual data points to produce two matrices: factor profiles and factor contributions. So PMF can be written as:

$$x_{ij} = \sum_{k=1}^{p} g_{ik} f_{kj} + e_{ij}$$
 (1)

where x_{ij} is the measured concentration of compound j in sample i ($\mu g \ m^{-3}$), p is the total number of factors, g_{ik} is the contribution of factor k to sample i ($\mu g \ m^{-3}$), f_{kj} is the profile of compounds j of

factor $k\,(g\,g^{-1})\!$, and e_{ij} is the residual for the compounds j in sample i $(\mu g\,m^{-3})\!$.

The aim of the PMF method is to find the minimum weighted sum of the squared residual function Q value (Equation (2)) by using least-squares fitting (Paatero and Tapper, 1993, 1994). The solution obtained at the minimum Q value is considered to be a reasonable result. The equation is as follows:

$$Q = \sum_{i=1}^{n} \sum_{j=1}^{m} \left[\frac{x_{ij} - \sum_{k=1}^{p} g_{ik} f_{kj}}{u_{ij}} \right]^{2}$$
 (2)

Here, u_{ij} is the uncertainty of x_{ij} , n is the total number of samples, and m is the total number of measured compounds. The value of p, m, and n are restricted as p < m and n > m. More details about PMF are described by previous studies (Paatero and Tapper, 1993; Paatero and Hopke, 2003; Reff et al., 2007; Norris et al., 2008).

Input data x_{ij} lower than or equal to the limit of quantification (LOQ) were replaced by half of the LOQ and their uncertainties u_{ij} were set as 5/6 of the LOQ (Polissar et al., 1998). But if x_{ij} is higher than the LOQ, u_{ij} were calculated by following equation (Norris et al., 2008):

$$u_{ij} = \left(\left((\text{Error Fraction})*x_{ij}\right)^2 + \text{LOQ}_{ij}^2\right)^{0.5} \tag{3}$$

where error fraction (%) is estimated from both sampling error and analytical error. In this study, an error fraction of 8–10% for trace elements, 8% for EC and OC, 12–15% for water soluble ions, and 12–20% for organic compounds were estimated for the PMF analysis.

The missing data were replaced by the mean values of that species and the uncertainties were set as three times of the mean value (Gu et al., 2011). LOQ of all species are shown in the Table S1 of the Supporting Material. The modeling uncertainty, which is caused by other errors, such as variation of source profile and chemical transformation, was set as 5% in this study according to the suggestion from Norris et al. (2008).

In this study, species were discarded from the model if the sum of the number of missing data and the number of data with values below the LOQ was more than 1/3 of the samples.

Signal to Noise (S/N) ratios were used to categorize a species, and according to S/N ratios (Paatero and Hopke, 2003), three categories were obtained: "bad" (S/N < 0.2), "weak" (0.2 < S/N < 2), and "strong" (S/N > 2). "Bad" means this species will be excluded from the PMF model. "Weak" means the uncertainty of this species will be increased by model in order to reduce the influence of this species. Further information about S/N ratios of each input species are listed in Table S2 of the Support Material. 321 PM samples with 31 species (OC, EC, Cl⁻, NO₃, SO₄²-, NH₄, K, Ca, Ti, Mn, Fe, Cu, Zn, As, Ba, Pb, 29ab, 29ba, 30ab, 30ba, 31abS, 31abR, BAA, CRY, BBKF, BEP, BAP, IND, PIC, BGH and levoglucosan) were used in the final PMF analysis (n = 321 and m = 32). The PM₄ mass concentration was also included but marked as a "total variable" which was grouped into the "weak category" automatically by the model in order to reduce its influence on the PMF solution. PMF was run several times with different factor numbers (4-12) to determine the most reasonable number of factors. The Q values (see equation (2)), which are goodness-of-fit parameters, are checked first to assess how well the model fits. The O values in all runs converged and Orobust was close to Q-true, indicating that the model fit well with the input data and the global minimum Q was found. In addition, the G-space plot (factor versus another factor) showed no edges in all factors, indicating that there is no rotational ambiguity. Therefore Fpeak = 0 was used in this study. Finally, six factors were determined to be the most meaningful result. After a reasonable solution was selected, a 100 bootstrap was run (minimum $R^2 = 0.6$) to check its stability. Of the 100 runs, factor 1, factor 2 and factor 6 only had 2, 2 and 3 bootstraps unmapped, respectively, while all the remaining three factors had all bootstraps mapped. The correlation R² between modeled PM₄ mass concentrations by PMF and measured PM₄ mass concentrations reached 0.93 with a slope of 0.96, showing that model can adequately reproduce the measured PM₄ mass concentration. Therefore, the solution with six factors was considered as a stable result.

2.5. Backward trajectory analysis

The HYSPLIT4 (Hybrid Single Particle Lagrangian Integrated Trajectory, Version 4) model was used to calculate backward trajectories of air flows (http://ready.arl.noaa.gov/HYSPLIT.php) with meteorological data from Global Data Assimilation System (GDAS). In order to cover both horizontal and vertical scale transport of air flows, 72 h backward trajectories were selected (Zhu et al., 2011; Li et al., 2012b). 500 m height above ground level (AGL) at the ending point was chosen because in general pollutants are well mixed up to this height. The same application can also be found in previous studies (Zhang et al., 2009b; Ji et al., 2014). The time ending at 06:00 UTC (14:00 local) was chosen for calculating backward trajectories indicative of each day because the MLH is the highest at this time during the day and the conditions are favorable for mixing of air pollutants.

In order to obtain the possible source locations, cluster analysis based on backward trajectories was performed by multiple iterations. The aim of cluster analysis is to sort all backward trajectories which have similar movements into the same group, a so-called

cluster. During iteration, the cluster spatial variance (SPVAR) and the total spatial variance (TSV) among trajectories were calculated. SPVAR is the sum of the squared distances between the endpoints of the trajectories and corresponding cluster-mean, while TSV is the sum of SPVAR of all clusters (Draxler et al., 2009). At the initial step, one trajectory is considered as one cluster. With iterations, two trajectories with the lowest increase in STV are paired into the same cluster. Iterations continue until the rapid increase in STV is found. The detail about cluster analysis can be found in previous studies (Draxler et al., 2009; Kelly et al., 2012).

2.6. Quality assurance/quality control (QA/QC)

All filter holders and rings were cleaned by de-ionized water twice in an ultrasonic bath before being used. A time of 20 min was used for each cleaning. The holders and rings were then washed by de-ionized water individually once more and baked at 110 °C in an oven for 1 h. The tweezers were also first cleaned by de-ionized water and then by methanol once more before each time using. All loaded filters were stored at -20 °C before the chemical analysis, while all experimental results were corrected by deducting the blank filter values.

A not instantly perceived fault during installation of the devices led to a decreased collection air flow of 167 l min⁻¹ in both samplers. Meanwhile, the size of the collected particles on the filters was changed with the reduction of flow volume of samplers.

According to the impactor design theory (Gussman, 1969; Marple and Liu, 1974; Marple and Willeke, 1976), the equation is given as:

$$Stk_{50} = \frac{4\rho_p QCD_{50}^2}{9\pi n \mu W^3} \tag{4}$$

Here, Stk₅₀ is the stokes number at 50% collection efficiency, ρ_p is the particle density ($\rho_p=1~g~cm^{-3}$), Q is the total volume passing through the sampler, C is the Cunningham slip correction factor, D₅₀ is particle diameter at 50% collection efficiency, n is the number of nozzles (n = 10), μ is the flux viscosity ($\mu=1.81\times10^{-4}~kg~s^{-1}~m^{-1}$) and W is the jet width (5.6 mm).

Because Stk_{50} is relatively constant when the ratio of jet-to-plate distance to jet width (S/W) is larger than 1.0 (Marple and Willeke, 1976) (in our study, S/W = 3.6), the cut-off size of particles $C^{0.5}D_{50}$ can be recalculated as PM_4 (aerodynamic diameter of PM is less than 4 μ m), which is still meaningful and can be represented as respirable particulate matter (Fromme et al., 2005; Keil et al., 2010). The most important point is that the variation trend of PM_4 is supported by simultaneous $PM_{2.5}$ TEOM data at CAS/IAP (Institute of Atmospheric Physics, Chinese Academy of Sciences) (Xin et al., 2014).

3. Results

3.1. PM₄ mass concentrations

Annual variation of PM₄ mass concentrations from 18 to 321 μ g m⁻³ with an annual average value of 83 μ g m⁻³ is shown in Fig. 2. Significant variation of monthly PM₄ mass concentrations was observed. PM₄ mass decreased continuously from June 2010 till September 2010, then increased from October 2010 till November 2010, and decreased again after December 2010, reached the lowest monthly average value (44 μ g m⁻³) in January 2011, and the highest monthly average value of 117 μ g m⁻³ in April 2011 (Fig. S1 of the Supporting material). The seasonal variation of PM₄ mass concentration was also examined. Considering the heating periods, the seasons are defined as summer from June till August, autumn in

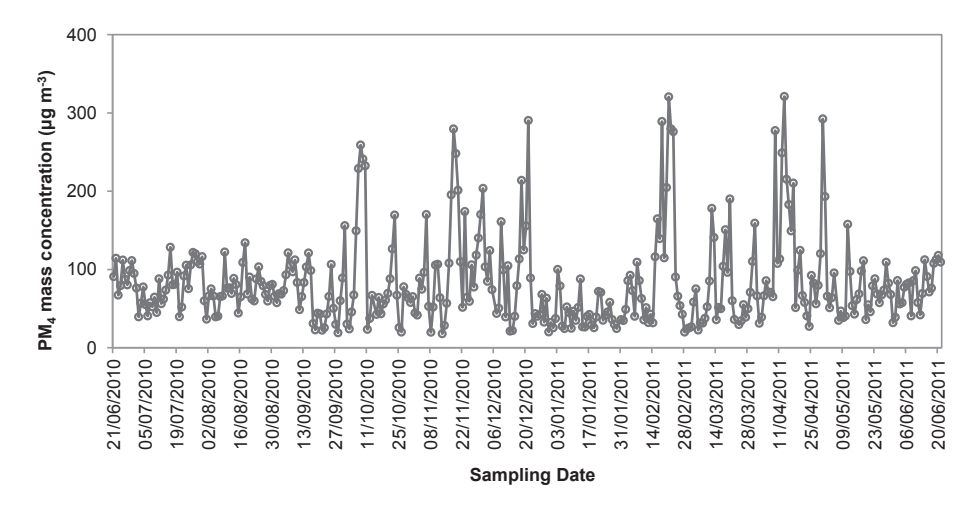


Fig. 2. Annual variation of daily mean PM_4 mass concentrations at the CUGB from 2010.06.21 till 2011.06.20.

September and October, winter from November till March, and spring in April and May. Only 20 days were investigated in summer 2011 (from 1 June till 20 June 2011), which cannot be representative for summer 2011. So in this paper, the data of these 20 samples will not be discussed with respect to seasonal variation. PM₄ mass concentrations are found to reach the highest value of 95 $\mu g \ m^{-3}$ during spring 2011, decrease through the winter 2010 (83 $\mu g \ m^{-3}$), summer 2010 (82 $\mu g \ m^{-3}$) and show the lowest values in autumn 2010 (80 $\mu g \ m^{-3}$).

3.2. Mass concentrations of chemical species in PM₄

In order to assess air quality, seasonal average mass concentrations of chemical compounds in PM_4 are listed in Table 1.

3.2.1. EC and OC

The variation of daily EC and OC are shown in Fig. S2(a) of the Supporting material. Daily EC and OC mass concentrations varied from 0.5 to 11.6 μ g C m⁻³ and from 5.4 to 70.1 μ g C m⁻³ with annual average mass concentrations of 3.8 \pm 2.1 (mean \pm standard deviation, similarly hereinafter) μ g C m⁻³ and 18.9 \pm 10.9 μ g C m⁻³, respectively. EC had the highest mass concentration in autumn 2010 (4.3 \pm 2.2 μ g C m⁻³) and the lowest mass concentration in spring 2011 (3.2 \pm 1.8 μ g C m⁻³), while the seasonal average concentration of OC was the highest of 19.2 \pm 13.5 μ g C m⁻³ in winter 2010 and the lowest of 18.0 \pm 9.7 μ g C m⁻³ in spring 2011. The mass percentages of EC and OC in PM₄ showed no large variation in different seasons, 5.2%, 5.9%, 5.4% and 4.3% for EC and 26%, 26%, 25% and 24% for OC in summer 2010, autumn 2010, winter 2010 and spring 2011, respectively. The annual average contributions of EC and OC to PM₄ mass were 5.3% and 26%, respectively.

Carbonaceous matter (CM) was estimated applying the following equation (Turpin and Lim, 2001).

$$CM = OM + EC = 1.6 \times OC + EC$$
 (5)

where OM is organic matter which can be estimated from OC. The ratio between OM and OC was found to range from 1.4 to 1.8 depending on the oxidative state of the aerosol which may lead to a seasonally dependent ratio. In this study, an average ratio of 1.6 was used (Turpin and Lim, 2001).

CM contributed 45%, 48%, 46% and 38% to PM_4 mass in summer 2010, autumn 2010, winter 2010 and spring 2011, respectively with the annual average mass percentage of 46%. It shows that CM is an important constituent in PM_4 .

A ratio of OC/EC higher than 2 is an indicator for the presence of secondary organic carbon (SOC) (Chow et al., 1996). OC/EC mass ratio in Fig. S2(a) of the Supporting material showed that all OC/EC ratios during the whole year were higher than 2, which indicated that SOC formation in Beijing PM is common. SOC can be estimated from OC and EC but an uncertainty is exists which is not easily evaluated. Therefore, estimation of SOC was not conducted in this study. OC/EC ratios varied from 2.7 to 48.6 with an average value of 5.3. The seasonal variation showed that the lowest OC/EC ratio was 4.4 in autumn 2010 and the highest value was 5.6 in spring 2011. The highest OC/EC value (48.6) was found on 1 May 2011 caused by dust storm on 1 May 2011 which transported organic soil material with high OC concentration (Zhao et al., 2013a) to Beijing.

3.2.2. Organic compounds

Levoglucosan shown in Fig. 2S(b) of the Supporting material was the dominant compound in all measured organic species and mass concentrations varied from 8 to 2443 ng m $^{-3}$ with an annual average value of 406 ng m $^{-3}$ and contributed 0.6% to PM₄ mass. The seasonal variation of levoglucosan mass concentration (Table 1) showed the highest mass concentration in summer 2010 (667 ng m $^{-3}$), followed by autumn 2010 (568 ng m $^{-3}$), winter 2010 (369 ng m $^{-3}$), and the lowest was in spring 2011 (176 ng m $^{-3}$).

Most of hopanes, except Ts, 30ab and 31abS, had the highest mass concentration in winter 2010 (Table 1). The dominant substances were 29ab and 30ab in all hopane compounds (Fig. 2S(b)), which contributed 23% and 24% to the hopane pattern, respectively.

The daily sum of PAH mass concentrations were in the range of $1-332~\rm ng~m^{-3}$. The lowest PAH mass concentration was found in summer 2010, followed by spring 2011 and autumn 2010, and increased rapidly during winter time as also observed in previous studies (He et al., 2006; Huang et al., 2006).

3.2.3. Water soluble ions

 SO_4^{2-} showed the highest mass concentration of 21.9 $\mu g \ m^{-3}$ in summer 2010 and the lowest mass concentration of 9.9 $\mu g \ m^{-3}$ in spring 2011. NO_3^- had the highest mass concentration at 11.7 $\mu g \ m^{-3}$ in winter 2010 and the lowest mass concentration in summer 2010 (1.7 $\mu g \ m^{-3}$). Seasonal variation of NH_4^+ mass concentration showed the highest value in autumn 2010, followed by summer 2010, winter 2010, and spring 2011. The contribution of SO_4^{2-} , NO_3^- and NH_4^+ (SNA) to PM₄ mass concentration ranged from 2% to 85% with an annual average value of 24%, and 33%, 26%, 23% and 20% in summer 2010, autumn 2010, winter 2010 and spring 2011,

 Table 1

 Seasonal average mass concentrations of chemical compounds in PM4 at the CUGB from 2010.06.21 till 2011.06.20 (unit: from EC to NH4: μ g m⁻³; from Fe to COR: ng m⁻³).

Species	Annual average	Summer 2010	Autumn 2010	Winter 2010	Spring 2011
EC/OC		·			
EC	3.8 ± 2.1	3.8 ± 0.9	4.3 ± 2.2	4.0 ± 2.6	3.2 ± 1.8
OC	18.9 ± 10.9	18.2 ± 2.8	18.8 ± 10.6	19.2 ± 13.5	18.0 ± 9.7
Ions					
Cl ⁻	2.0 ± 3.0	0.07 ± 0.2	0.5 ± 0.7	3.0 ± 3.5	0.9 ± 1.7
NO_3^-	8.6 ± 21.2	1.7 ± 1.0	9.9 ± 17.4	11.7 ± 28.8	7.5 ± 11.3
SO ₄ ² -	12.8 ± 19.3	21.9 ± 16.3	12.8 ± 16.3	10.9 ± 23.7	9.9 ± 10.7
NH4	4.6 ± 8.6	5.6 ± 4.3	5.8 ± 9.9	4.6 ± 10.6	2.8 ± 4.0
Elements					
Fe	1455 ± 1198	1155 ± 368	1227 ± 605	1494 ± 1169	2103 ± 2013
K	1569 ± 1740	1163 ± 827	1070 ± 771	1899 ± 2318	1585 ± 1370
Ca	2340 ± 2048	1534 ± 544	1747 ± 862	2540 ± 1898	3587 ± 3494
Ti	102 ± 101	67.3 ± 22.9	72.6 ± 36.8	107 ± 77.6	175 ± 190
Mn	52.3 ± 37.4	37.6 ± 13.1	46.8 ± 23.3	61.0 ± 42.8	60.7 ± 48.9
Cr	16.3 ± 13.0	17.5 ± 11.0	14.3 ± 8.7	17.8 ± 15.5	14.3 ± 11.4
Ni	1.0 ± 0.7	0.9 ± 0.6	0.7 ± 0.5	1.1 ± 0.8	1.0 ± 0.7
Cu	35.5 ± 30.9	28.8 ± 16.8	37.0 ± 28.3	39.9 ± 37.8	31.0 ± 27.5
Zn	326 ± 301	350 ± 219	328 ± 296	313 ± 351	326 ± 295
As	15.6 ± 19.6	13.1 ± 13.1	12.7 ± 13.4	17.2 ± 24.6	16.8 ± 19.9
Sn	5.3 ± 3.6	5.0 ± 3.5	4.1 ± 3.3	5.3 ± 3.5	6.0 ± 3.8
Sb	2.8 ± 1.9	2.6 ± 2.0	2.7 ± 2.0	3.0 ± 2.0	2.7 ± 1.8
Ba	22.5 ± 18.8	17.8 ± 5.8	18.9 ± 9.5	23.1 ± 18.4	32.6 ± 31.5
Pb	105 ± 98.8	96.6 ± 56.2	97.3 ± 80.6	116 ± 122	99.2 ± 103
Organic compounds					
Levoglucosan	406 ± 352	667 ± 462	568 ± 451	369 ± 262	176 ± 131
Hopanes					
Ts	1.5 ± 1.0	1.5 ± 0.9	1.7 ± 0.9	1.3 ± 0.9	1.5 ± 0.9
Tm	2.4 ± 2.2	1.1 ± 0.5	1.6 ± 0.8	3.4 ± 2.7	1.3 ± 0.6
29ab	5.6 ± 4.2	4.6 ± 1.6	5.3 ± 2.3	6.6 ± 5.5	3.4 ± 1.9
29ba	2.9 ± 3.2	0.9 ± 0.5	1.3 ± 0.5	4.5 ± 3.7	0.9 ± 0.8
30ab	5.6 ± 3.7	5.2 ± 1.8	6.0 ± 2.5	5.7 ± 4.4	4.0 ± 2.7
30ba	2.6 ± 3.0	0.8 ± 0.3	1.4 ± 0.5	4.0 ± 3.6	0.9 ± 0.6
31abS	2.1 ± 1.1	2.3 ± 0.6	2.4 ± 0.8	1.9 ± 1.1	1.5 ± 0.9
31abR	1.9 ± 1.1	1.7 ± 0.4	1.7 ± 0.6	2.2 ± 1.4	1.2 ± 0.9
32abS	1.6 ± 0.9	1.4 ± 0.4	1.6 ± 0.4	1.8 ± 1.0	1.0 ± 0.9
32abR	1.4 ± 0.9	1.3 ± 1.0	1.1 ± 0.4	1.5 ± 0.9	0.9 ± 1.0
PAHs					
BAA	2.1 ± 4.0	0.1 ± 0.1	0.4 ± 0.4	4.4 ± 5.1	0.3 ± 0.2
CRY	5.6 ± 8.6	0.8 ± 0.4	1.9 ± 1.9	10.8 ± 10.8	1.4 ± 1.0
BBKF	7.5 ± 10.8	1.3 ± 0.5	3.6 ± 2.9	14.0 ± 13.5	2.2 ± 1.8
BEP	2.3 ± 3.3	0.4 ± 0.2	1.2 ± 0.9	4.2 ± 4.1	0.7 ± 0.6
BAP	2.6 ± 3.8	0.3 ± 0.2	1.1 ± 1.0	4.7 ± 5.0	1.2 ± 0.5
PER	0.7 ± 0.9	0.06 ± 0.03	0.4 ± 1.1	1.0 ± 0.9	0.2 ± 0.3
DAH	0.7 ± 0.8	0.00 ± 0.05 0.2 ± 0.1	0.4 ± 0.3	1.0 ± 0.5 1.1 ± 0.8	1.1 ± 1.3
IND	3.4 ± 4.4	0.2 ± 0.1 0.8 ± 0.5	0.4 ± 0.3 2.0 ± 1.4	5.9 ± 5.4	1.1 ± 1.5 1.3 ± 1.0
PIC	0.9 ± 0.8	0.0 ± 0.05	0.5 ± 0.3	1.2 ± 0.8	0.5 ± 0.5
BGH	2.5 ± 3.2	0.1 ± 0.03 0.6 ± 0.2	1.6 ± 1.2	4.3 ± 3.9	1.0 ± 0.9
COR	2.5 ± 3.2 2.6 ± 2.4	1.0 ± 0.8	1.4 ± 1.2	3.8 ± 2.6	1.0 ± 0.5 1.0 ± 0.8

respectively. Cl $^-$ was a minor fraction (2%) in PM $_4$ in comparison with SNA and it showed noticeably high mass concentration of 3.0 $\mu g \ m^{-3}$ during winter 2010 compared with summer 2010.

3.2.4. Inorganic elements

In all measured metals, Ca had the highest annual average mass concentration (2340 ng m $^{-3}$) while the lowest was Ni with 1.0 ng m $^{-3}$. Fe, Ca, Ti and Ba, which are discussed to be related to the crustal sources (Yang et al., 2005), accounted for 67% of all elemental mass, and showed similar variation patterns over the whole year with many similar peaks in mass concentration. For instance, the highest mass concentrations of these four elements occurred in spring 2011 which was likely due to a dust storm contribution (Fig. 3S(a) of the Supporting material). The annual average mass concentration of [Fe + Ca + Ti + Ba] was 3913 ng m $^{-3}$, and showed the seasonal average mass concentration of 2774, 3037, 4163 and 5898 ng m $^{-3}$ in summer 2010, autumn 2010, winter 2010 and spring 2011, respectively. The other non-crustal elements, such

as Zn, As and Pb, which are generally considered to originate from anthropogenic sources (Shi et al., 2010; Tian et al., 2010; Soriano et al., 2012; Xu et al., 2012), followed a similar pattern during the whole sampling period and showed no large differences from season to season ([Zn + As + Pb]: 460 ng m $^{-3}$ in summer 2010, 432 ng m $^{-3}$ in autumn 2010, 446 ng m $^{-3}$ in winter 2010 and 441 ng m $^{-3}$ in spring 2010) except significant lower mass concentrations in January 2011 (Fig. 3S(b) of the Supporting material), which corresponds to relatively low PM₄ mass concentration.

3.3. PM₄ mass balance

The mass balance of PM₄ is shown in Fig. 3. Organic matter was calculated by 1.6 times OC (Formula 5) and was the largest fraction of PM₄ with a mass contribution of 41%. SO_4^{2-} , NO_3^{-} and NH_4^{+} (SNA) contributed 25% to PM₄ mass. Crustal elements were described by the sum of Fe, Ca, Ti and Ba and contributed 5% to PM₄ mass. Trace elements including Cr, Ni, Zn, As, Pb, Sn, Cu and Sb, only were 1% of

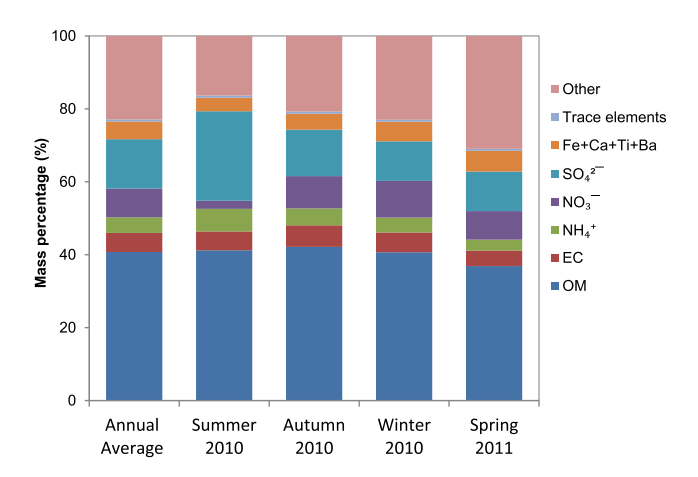


Fig. 3. Mass balance of PM_4 on the basis of daily mean samples in different seasons at the CUGB during 2010–2011.

 PM_4 mass. The other unknown part was the third highest fraction of PM_4 mass with the contribution of 23%.

Seasonal mass balance of PM $_4$ is also shown in Fig. 3. Both OM and EC had the lowest contribution of 37% and 4% to PM $_4$ in spring 2010, respectively. NO $_3$ showed the highest values (10%) in winter 2010 while SO $_4^{2-}$ and NH $_4^{+}$ had the highest contribution (25% and 6%) in summer 2010 on the contrary. The sum of Fe, Ca, Ti and Ba showed the clearly highest contribution in spring 2011 (6%). The exception was trace elements had no large variation during the four seasons.

3.4. Source apportionment

Six factors that can be explained as sources were determined by PMF (see discussion below). The species mass concentration (g g $^{-1}$, the species mass contained in 1 g particles in each factor) and mass percentage (%, the species mass concentration contained in one factor divided by the total mass concentration in all factors) are shown in Fig. 4. The time series variation of each factor mass concentration is shown in Fig. 5. The seasonal mass contributions of six factors are listed in Table 2.

4. Discussions

4.1. Organic compounds

Levoglucosan is widely used as an indicator for biomass burning (Zhang et al., 2008; Wagener et al., 2012), so the contribution of biomass burning to OC can be implied by the mass ratio of levoglucosan to OC (Zhang et al., 2008). Levoglucosan had much higher mass concentrations in summer and autumn than in winter and spring (Table 1), while the seasonal average mass ratios of levoglucosan to OC also showed the highest values in summer 2010 (0.04), followed by autumn 2010 (0.03), then winter 2010 (0.02) and spring 2011 (0.01). All these indicated that biomass burning contributed significantly to the particle loading in summer and autumn in Beijing. This agrees well with previous studies which pointed out that biomass burning, such as the combustion of agricultural waste and fallen leaves, usually happens in summer and autumn in Beijing and its surrounding area (Huang et al., 2012).

Fossil fuel combustion, such as coal combustion and vehicle emissions, is considered to be the main source of hopanes (He et al., 2006; Schnelle-Kreis et al., 2007). The hopane patterns, such as hopane index or homohopane index, are usually used to distinguish mineral oil based sources like vehicle emission from coal

combustion sources (Oros and Simoneit, 2000). The hopane index. 30ab/(30ab + 30ba), was found to be 0.1 for lignite coal, 0.5 for bituminous coal, 0.6 for brown coal (Oros and Simoneit, 2000) and greater than 0.9 for crude oil (El-Gayar et al., 2002). In this study, it varied from 0.29 to 0.95 with an annual average value of 0.72, and had the highest value of 0.86 in summer 2010, followed by autumn 2010 (0.83), spring 2011 (0.82) and the lowest values in winter 2010 (0.61). The homohopane index. 31abS/(31abS + 31abR), was found to be about 0.1 for lignite coal, 0.4 for bituminous coal, and 0.6 for fuel oil combustion (Oros and Simoneit, 2000; Schnelle-Kreis et al., 2007). In PM₄, it ranged from 0.14 to 0.78 with an annual average value of 0.53 and had a value of 0.57, 0.58, 0.47 and 0.56 in summer 2010, autumn 2010, winter 2010 and spring 2010, respectively. So both indexes in winter had lower values in comparison to other seasons, indicating that hopanes in spring, summer and autumn mainly originated from fuel oil consumption while coal combustion had a greater contribution to hopanes during winter.

PAHs had the highest mass concentrations in winter (Table 1). The reasons could be low temperatures, weak solar radiation (He et al., 2006) and the increase in coal combustion. PIC in PAHs, a tracer for coal combustion (Oros and Simoneit, 2000), had the highest mass concentration with the value of 1.2 ng m $^{-3}$ in winter 2010, followed by autumn 2010 and spring 2011 which had the same value of 0.5 ng m $^{-3}$ and much higher than in summer 2010 (0.1 ng m $^{-3}$). This supported that coal combustion contributed a large amount to PAHs during winter.

4.2. Interpretation of factors from PMF results

The first factor contained 65% of SO_4^{2-} , 50% of NH \ddagger and 55% of levoglucosan (Fig. 4). As discussed in Section 4.1, levoglucosan is widely used as a tracer for biomass burning (Zhang et al., 2008; Wagener et al., 2012). From Fig. 5 and Table 2, the time series variation and seasonal variation show that this factor had the highest mass concentration during summer (35.8 μ g m⁻³) and followed by autumn with the value of 13.7 μ g m⁻³. This is because biomass burning usually happens during summer and autumn in Beijing and its surrounding areas (Huang et al., 2012) and the secondary sulfate is easily formed under strong solar radiation and high temperature, especially in summer (Seinfeld and Pandis, 2006). In addition, previous studies showed that SO_4^{2-} mass concentration increased during biomass burning episodes (Cheng et al., 2014; Rastogi et al., 2014). Therefore this factor can be explained by biomass burning and secondary sulfate formation.

The second factor was characterized by high concentrations of nitrate and ammonium, which can be explained as a secondary nitrate formation. The time series (Fig. 5) and Table 2 show that this factor concentrated during autumn (13.2 $\mu g\ m^{-3}$) and winter (10.4 $\mu g\ m^{-3}$) but had the lowest concentration during summer (0.8 $\mu g\ m^{-3}$). The low values during summer may be biased because ammonium nitrate is semi-volatile and high temperatures in summer could have caused losses from the filters.

The third factor was mainly contributed by Fe (58%), Ca (59%), Ti (67%), Mn (48%), and Ba (59%) (Fig. 4). The main source of all these elements is considered as soil. The time series (Fig. 5) and seasonal variation (Table 2) showed that high concentrations of this factor were concentrated during spring with the value of 53.6 $\mu g~m^{-3}$ when dust storms occurred. For instance, this factor had a peak value on 30 April 2011 when a dust storm happened. Therefore, this factor is indicative of mineral dust, including dust storm, road dust and construction dust.

The fourth factor was characterized by relative high contributions of As (79%), Zn (66%), Pb (57%), Cu (45%) (Fig. 4). As was found to be originated from smelter and base-metal refinery industries (Wang and Mulligan, 2006). Zn and Cu are originated

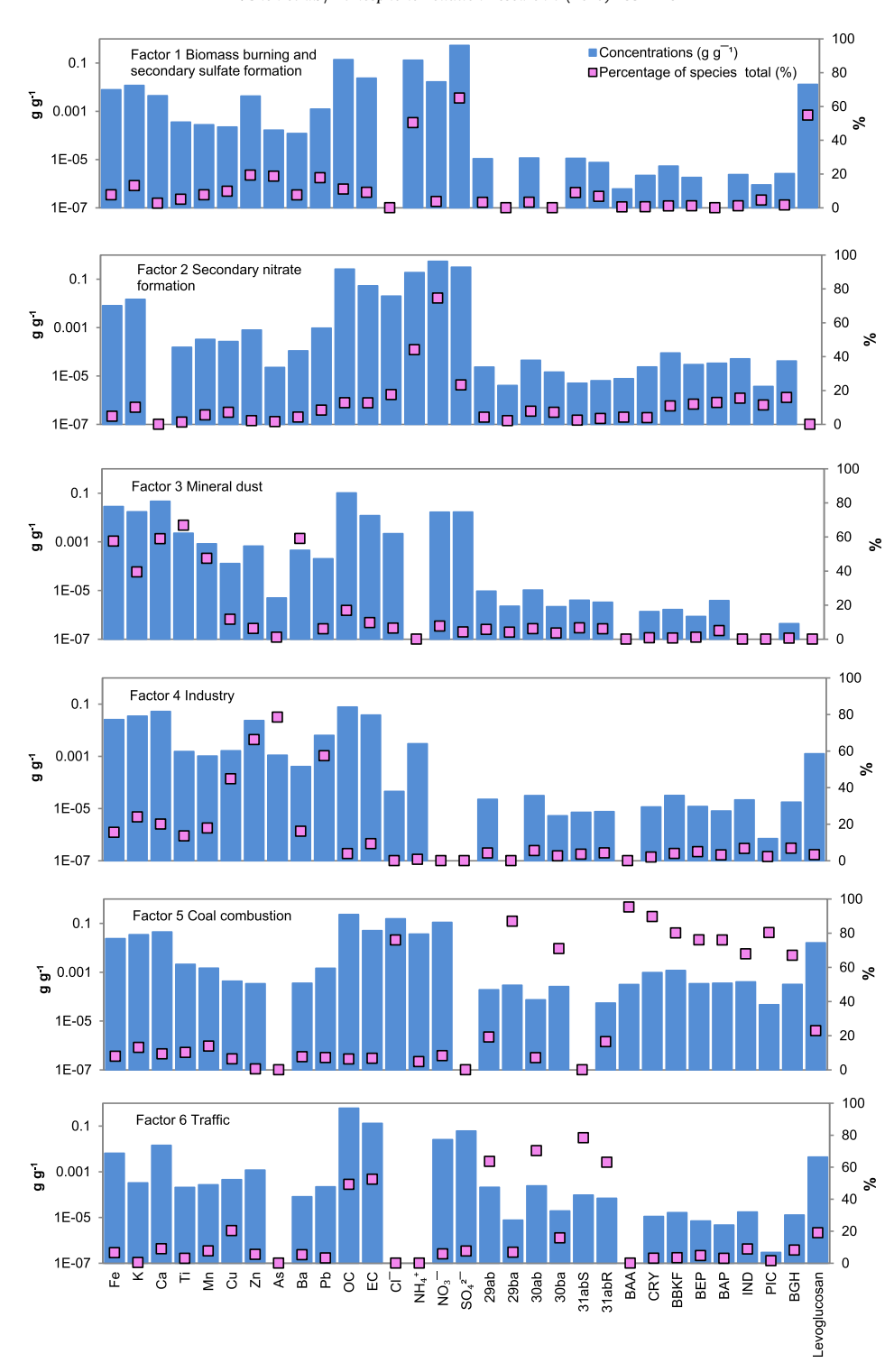


Fig. 4. PMF factor profiles from chemical compounds data in PM4 during 2010-2011 at the CUGB.

from industrial metallurgical process (Xu et al., 2012). Tangshan city and Tianjin Municipality are important industrial cities which are located to the Southeast of Beijing. The main industry in Tangshan is iron and steel. In Tianjin, metalworking is one kind of important industry. Pb was considered to have originated from the ceramic industry, the manufacturing of insecticides, paints, glass and storage batteries (Soriano et al., 2012). Porcelain is another important industry in Tangshan city and producing

photovoltaic cells is an important industry in Baoding city which is located to the Southwest of Beijing. In addition to surrounding cities, the smelter industry is also located inside of Beijing, to the Northwest of CUGB, which is called "Changping smelter". All above mentioned support that this factor can be representative of industrial based sources. The time series (Fig. 5) shows that the contribution of this factor to PM₄ is stable during the whole year, except in January 2011 where the lowest mass concentration was

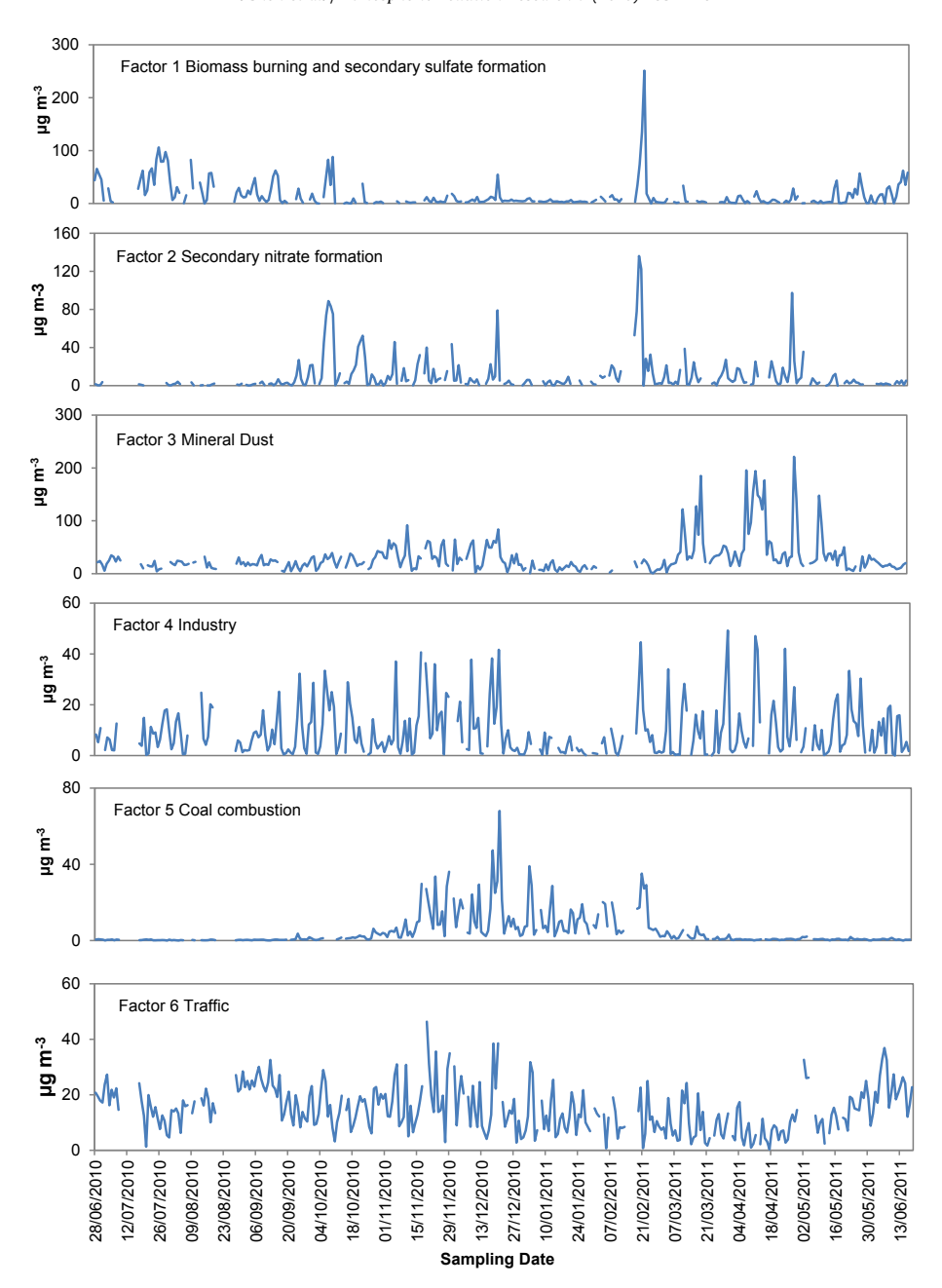


Fig. 5. Daily mean contributions of six sources from the PMF analysis for PM4 at the CUGB in Beijing during 2010–2011.

found, which is supported by the lowest PM_4 mass concentration at the same period. The reason could be it was influenced by meteorological parameters and the decrease in human activities during winter holiday period.

The fifth factor in Fig. 5 was dominated by PAHs (95% of BAA, 90% of CRY, 80% of BBKF, 76% of BEP, 76% of BAP, 68% of IND, 80% of PIC and 67% of BGH), 29ba (87%), 30ba (70%), Cl^- (76%), and levoglucosan (23%). Levoglucosan was found not only from biomass

Table 2 Seasonal contributions of 6 factors to PM_4 during 2010–2011 (unit: $\mu g\ m^{-3}$).

	Factor 1	Factor 2	Factor 3	Factor 4	Factor 5	Factor 6		
	Secondary sulfate formation and biomass burning	Secondary nitrate formation	Mineral dust	Industry	Coal combustion	Traffic		
Annual average	14.1	8.6	29.1	8.8	4.8	14.4		
Summer 2010	35.8	0.8	17.1	7.3	0.3	16.3		
Autumn 2010	13.7	13.2	20.7	9.0	1.1	17.5		
Winter 2010	8.6	10.4	27.7	8.9	10.2	13.4		
Spring 2011	8.5	8.1	53.6	9.9	0.7	9.8		

burning, but also from lignite combustion (Fabbri et al., 2008, 2009). Even though levoglucosan could also be caused by biomass burning for heating in winter, this form of heating is less common in the Beijing-Tianjin-Hebei region in comparison with coal combustion. Therefore, levoglucosan in this factor was most probably from coal combustion. Cl⁻ also can originate from coal combustion (Yao et al., 2002) and PIC is also used as a tracer for coal combustion (Oros and Simoneit, 2000). In this factor, the hopane index 30ab/(30 ab + 30ba) is 0.2. As discussed in Section 4.1, this factor can be interpreted as coal combustion. In addition, contribution of this factor was found to be concentrated during winter (Fig. 5 and Table 2), indicating that coal combustion for heating during winter is the main reason. Most of PAHs were found to have a high contribution in this factor, showing that most of the very health hazardous PAHs are associated with coal combustion.

The sixth factor found in Fig. 5 was characterized by EC (52%), OC (49%), 29ab (64%), 30ab (70%), 31abS (78%) and 31abR (63%). In this factor, the homohopane index 31abS/(31abS + 31abR) was 0.6 and the hopane index 30ab/(30ab + 30ba) was 0.9. Both indexes indicated that this factor can be explained by oil combustion. Hopanes are considered to be an organic tracer for the lubricating oil which is usually used for gasoline or diesel engine vehicles (Rogge et al., 1993; Phuleria et al., 2006; Kleeman et al., 2009). Therefore this factor can be considered as traffic.

The six factors can be interpreted as a mixture of secondary sulfate formation and biomass burning, secondary nitrate formation, mineral dust, industry, coal combustion and traffic. These sources contributed the average value of 14.1, 8.6, 29.1, 8.8, 4.8 and $14.4 \,\mu g \, m^{-3}$ to PM₄ mass and constitute 18%, 11%, 36%, 11%, 6% and 18% of PM₄ mass, respectively (Table 2). The major sources of PM_{2.5} in Beijing from previous studies (Song et al., 2007; Wang et al., 2008; Yu et al., 2013) can be listed as: dust, biomass burning, coal combustion, industry, vehicle emission and secondary particles formation. The difference to these studies is that the contribution of each source is different. In particular, the contribution of mineral dust to PM is much higher in this study and mineral dust is found to be an important source in Beijing, especially in spring. The reason could be that the size of PM₄ is coarser than PM_{2.5}. On the other hand, the sampler inlet tubes were installed at a height of 2 m above ground, which is a typical height for the exposure of humans and is closer to the ground which can be more influenced by road dust.

The results from source apportionment illustrate the seasonal variation of each source and the dominant source of PM in each season (Table 2). In general, secondary sulfate formation and biomass burning contributions were concentrated in summer, while secondary nitrate formation concentrated in autumn and winter. PM from mineral dust had a relative high concentration during the whole year, especially in spring. Industry distributed relatively consistently throughout the whole year. Coal combustion for heating clearly had an obvious high contribution in winter. PM from traffic had a relative higher concentration in summer and autumn.

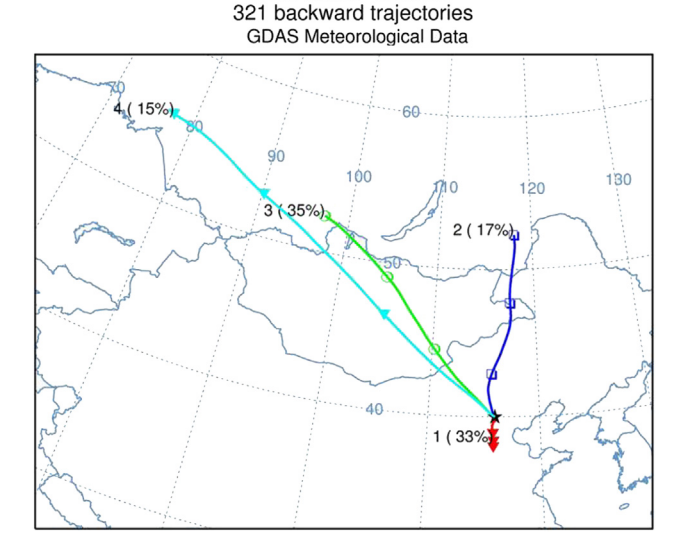
Considering source markers usually have more than one possible source, using single source marker or one category of species to trace the source is not complete. In this study, source apportionment was performed using a full year of data from both of inorganic and organic species for the first time to obtain more reasonable source identifications. In doing so it was possible to identify contributions from, e.g., coal combustion separated from traffic emissions. On the other hand it was not possible to un-mix sources with very similar variations in time like secondary sulfate formation and biomass burning.

4.3. Regional transportation indicated by back trajectories and cluster analysis

HYSPLIT4 was used to calculate 72 h backward trajectories at 500 m AGL prior to arriving in Beijing at 14:00 local time each day. Four trajectory clusters were obtained (Fig. 6).

Clusters 1, 2, 3 and 4 expressed the air flow from the South, the North, the Northwest and the Northwest with a long range transport of Beijing, respectively. These clusters are called the "South flow" (S flow), the "North flow" (N flow), "Northwest flow" (NW flow) and Long-range Northwest flow" (Long-range NW flow) and they accounted for 33%, 17%, 35% and 15% of all air flows, respectively. Long-range NW flow was longer than NW flow which indicated that Long-range NW flow had higher wind speeds in comparison with NW flow. In all clusters, the S flow was the shortest trajectory by far, which can be explained by the presence of relatively stagnant conditions.

According to these four clusters, all sampling days were also classified into four groups (Table 3). The highest PM4 mass concentration was from the S flow (103 μ g m⁻³), followed by the longrange NW flow (95 $\mu g \ m^{-3}$), the NW flow (63 $\mu g \ m^{-3}$) and the N flow (57 μ g m⁻³). The mixture of secondary sulfate formation and biomass burning, secondary nitrate formation and industry sources were mainly from S flows with the highest mass concentrations of 33.5, 14.2 and 12.8 $\mu g\ m^{-3}$, respectively. In other words, the precursors of secondary inorganic ions, such as SO₂ and NO_x, were transported mainly from the cities which are located in the South of Beijing, such as Tianiin Municipality and Tangshan city. Both of these two cities are important heavy industrial cities. This indicates that cities located in the South of Beijing play an important role in PM pollution in Beijing. The highest contributions from mineral dust (43.9 μ g m⁻³) and coal combustion (10.8 μ g m⁻³) were found to be from long-range NW flows, the longest trajectory, which means this cluster was accompanied by the highest wind speed. In addition, this air flow passed Russia, Mongolia, Inner Mongolia and Hebei Province to Beijing. Therefore, high wind speeds could transport the dust particles from Gobi desert in Mongolia and sandy lands in Inner Mongolia to Beijing, leading to the increase in the mass concentration of mineral dust. Coal is widely used for heating during winter in Mongolia, Inner Mongolia and Hebei



Cluster means - Standard

Fig. 6. Clusters of backward trajectories during 2010–2011.

Table 3 Summary of source distribution to PM_4 and corresponding PM_4 mass concentration on different directions of air flows during 2010–2011 (unit: $\mu g m^{-3}$). S is South, etc.

Direction	Secondary sulfate formation and biomass burning	Secondary nitrate formation	Mineral dust	Industry	Coal combustion	Traffic	PM ₄
S flow	33.5	14.2	22.6	12.8	3.3	16.7	103
N flow	5.5	5.9	23.6	6.6	2.5	12.6	57
NW flow	3.4	4.7	31.6	5.9	4.7	13.0	63
Long-range NW flow	6.9	8.8	43.9	9.5	10.8	15.1	95

Province, and Zhangjiakou fossil-fuel power station, which mainly used coal, is also located on route where the long-range NW flow passed. 75% of sampling days from long-range NW flows were found to be in winter. Therefore, the highest contribution from coal combustion was found from long-range NW flows coincidentally. Traffic showed little variation in all four backward trajectory clusters, indicating that it was mainly from local sources.

4.4. Influences of meteorological parameters and effect on visibility

Previous studies have pointed out that meteorological parameters were key factors affecting PM loading (Schäfer et al., 2006, 2011, 2014; Deng et al., 2012). The correlation coefficients between PM₄ and meteorological parameters such as T, WS, RH and MLH are listed in Table S3 of the Supporting Material.

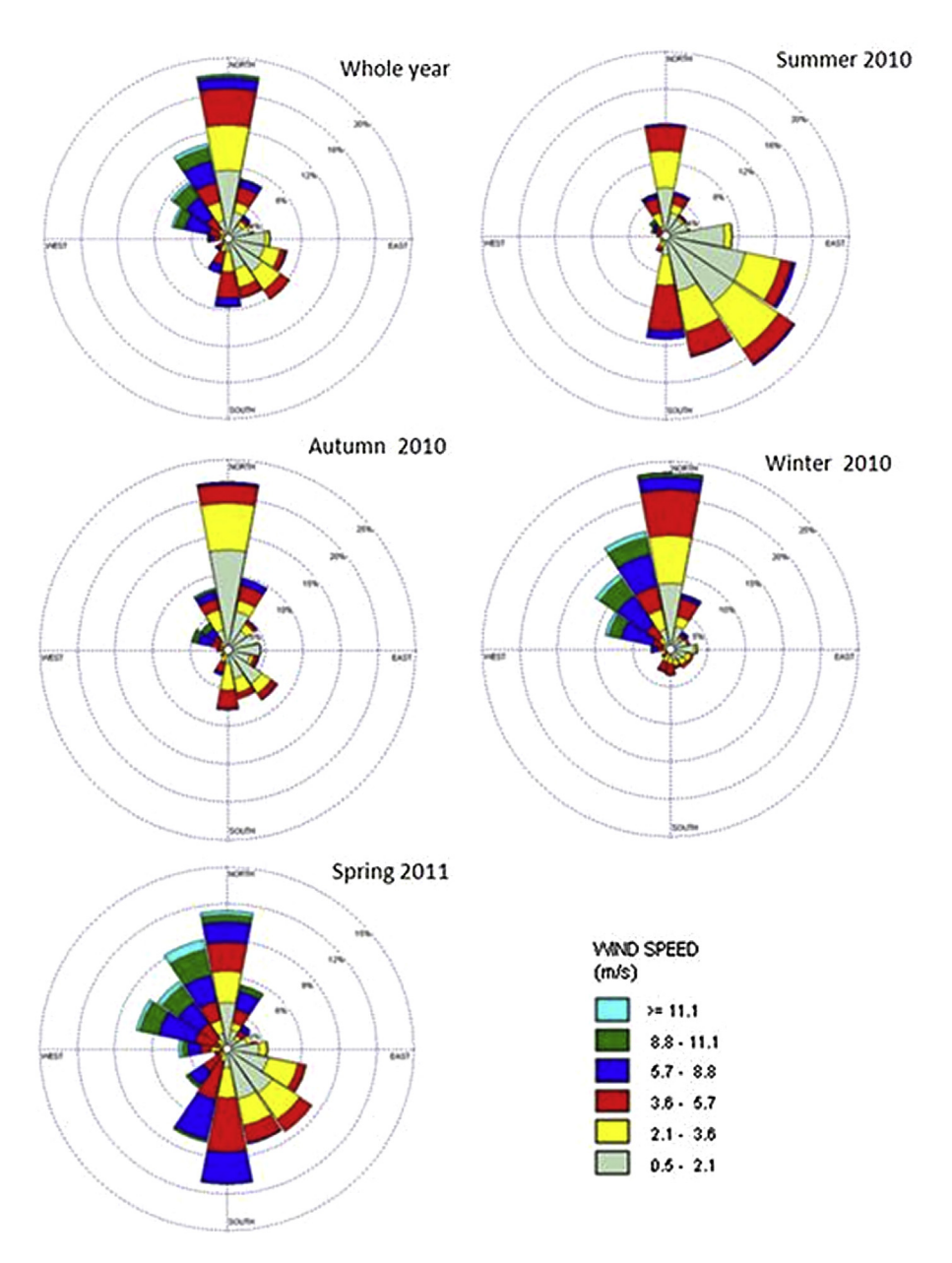


Fig. 7. Wind rose (WRPLOT View Freeware, Lakes Environmental, Canada) for PM4 sampling at the CUGB, Beijing (data obtained from ZBAA) from half hourly mean data during different seasons.

Temperature had no significant correlation with PM₄ and most of its compounds except Cl $^-$, all PAHs, Tm, 29ba and 30ba. Coal combustion for heating is one important source of Cl $^-$ (Yao et al., 2002) and PAHs. Therefore, it was expected that the decrease in ambient temperatures may lead to the increase in coal combustion and increasing contribution from related emission constituents to PM in Beijing. On the other hand, stronger solar radiation accompanied by higher temperatures can accelerate the photochemical degradation of PAHs.

RH had a weakly positive correlation with PM₄ mass concentrations which indicated a high RH could favor the growth of the particles. This could be caused by hygroscopicity of particles which can lead to the increase in PM mass concentration. Especially, EC, NH $^{\perp}$, SO $^{2-}$, Zn, 31abS and levoglucosan were found to have a positive correlation with RH. EC contains char and soot (Han et al., 2009), and aged soot is hydrophilic (Niu et al., 2011).

Generally, wind speed had a negative correlation with PM₄ mass concentration and almost all compounds which supported that high wind speed could enhance the dispersion of pollutants. However in some cases, a high wind speed can also cause high PM mass concentration, such as a dust storm. Therefore, the threshold value of wind speed should be considered. In this study, this threshold cannot be determined because the influence on PM is often inferred from other meteorological parameters.

The MLH was found to have a negative correlation with PM₄ and most compounds which illustrated that a lower MLH could accelerate the accumulation of pollutants from local and regional sources.

Wind direction and precipitation are other two very important factors for influencing PM mass concentrations in Beijing. The wind conditions in this study are shown in Fig. 7. In spring, the prevailing wind directions were from the North, Northwest, South and Southeast. Therefore, dust storms which were from north and northwest can bring more particles into Beijing and then cause particularly higher PM concentrations in spring than in other seasons. In winter, the dominant wind direction was blown from the North and brought fresh air into Beijing, thus leading to PM4 mass concentration during winter lower than during spring. In summer and autumn, the PM4 concentration was relatively low because 59% and 30% of precipitation happened during these two seasons which can cause the wet deposition of particles leading to the decrease in PM mass concentration.

Visibility had negative correlations with all chemical compounds, especially strong negative correlations with PM, OC, EC, SO_4^{2-} , NH_4^+ , Cu, Zn, Pb and levoglucosan, which meant visibility decreased with the increase in the PM mass concentration and is highly correlated with anthropogenic compounds. In addition, visibility was also significant affected by RH (correlation coefficient R=-0.70).

5. Conclusions

The temporal variations of PM and its compounds were investigated and the results showed that the PM mass concentrations at the height for exposure of humans after the emission reduction measures during the Olympic Summer Games 2008 were still high with an average value of 83 $\mu g \ m^{-3}$, which is much higher than annual average of Chinese Ambient Air Quality Standard for PM_{2.5} (Grade II: 35 $\mu g \ m^{-3}$) (China State Environmental Protection Administration (SEPA), 2012). The influence of PM on human health is still serious.

The mass balance showed that OM and SNA were two major fractions of PM in Beijing during the whole year with the contribution of 41% and 25% to PM mass, respectively, which means anthropogenic PM is a very important part of the total PM.

Sources of PM were obtained by performing source apportionment, using PMF. They were industry, secondary nitrate formation, secondary sulfate formation, coal combustion, traffic, dust and biomass burning. These results were totally supported by the analysis of seasonal variation and characteristics of chemical species.

The seasonal variation of different sources points out the dominant source in each season: secondary sulfate formation, biomass burning contributions and secondary nitrate formation in summer, secondary nitrate formation in autumn, mineral dust in spring and coal combustion in winter. This is helpful for policy makers for the purpose of improving air quality according to the corresponding dominant PM source in each season.

Regional transportation can contribute significantly to the air pollution in Beijing. Backward trajectories, in combination with cluster analysis, demonstrated that the southerly air flow (S flow) is responsible for the high SNA and emission from the biomass burning and industry and it is the direction which transported the most PM to Beijing.

Meteorological parameters were the important factors influencing PM and its compound mass variations. In general, high relative humidity and low MLH can raise PM mass concentration, while high wind speed and precipitation can reduce pollutants. In addition, wind direction also plays a key role in influencing PM because different wind directions can bring different pollutants to Beijing from different regions.

Conflict of interest

There is no conflict of interest.

Acknowledgment

The authors greatly thank Prof. Kuang Cen of the School of Earth Sciences and Resources of the China University of Geosciences (CUGB) for organizing the sampling site. Thanks to Jing Wang and Jianying Wang of the China University of Mining and Technology (CUMTB) for assisting with collecting PM samples for one year. We also thank MSc. Regula Muther, Digitel, for cooperation during QA/QC work. Chemical analyses at the Helmholtz Zentrum München were carried out in the framework of the Helmholtz Virtual Institute Institutes Complex Molecular Systems in Environmental Health (HICE). This work is supported by scholarships of the China Scholarship Council (CSC), the KIT Centre for Climate and Environment and the National Natural Science Foundation of China under No. 41175109.

Appendix A. Supplementary data

Supplementary data related to this article can be found at http://dx.doi.org/10.1016/j.apr.2015.09.008.

References

Cao, J.J., Wang, Q.Y., Chow, J.C., Watson, J.G., Tie, X., Shen, Z., Wang, P., An, Z., 2012. Impacts of aerosol compositions on visibility impairment in Xi'an, China. Atmos. Environ. 59, 559–566.

Cheng, Y., Engling, G., He, K.B., Duan, F.K., Du, Z.Y., Ma, Y.L., Liang, L.L., Lu, Z.F., Liu, J.M., Zheng, M., Weber, R.J., 2014. The characteristics of Beijing aerosol during two distinct episodes: impacts of biomass burning and fireworks. Environ. Pollut. 185, 149–157.

China State Environmental Protection Administration of China. Ambient Air Quality Standard of People's Republic of China (GB3095-2012).

Chow, J.C., Watson, J.G., Chen, L.W.A., Chang, M.C.O., Robinson, N.F., Trimble, D., Kohl, S., 2007. The IMPROVE_A temperature protocol for thermal/optical carbon analysis: maintaining consistency with a long-term database. J. Air Waste Manag. Assoc. 57, 1014–1023.

- Chow, J.C., Watson, J.G., Lu, Z.Q., Lowenthal, D.H., Frazier, C.A., Solomon, P.A., Thuillier, R.H., Magliano, K., 1996. Descriptive analysis of PM2.5 and PM10 at regionally representative locations during SJVAQS/AUSPEX. Atmos. Environ. 30, 2079—2112.
- Deng, X.L., Shi, C.N., Wu, B.W., Chen, Z.H., Nie, S.P., He, D.Y., Zhang, H., 2012. Analysis of aerosol characteristics and their relationships with meteorological parameters over Anhui province in China. Atmos. Res. 109–110, 52–63.
- Dimitrova, R., Lurponglukana, N., Fernando, H.J.S., Runger, G.C., Hyde, P., Hedquist, B.C., Anderson, J., Bannister, W., Johnson, W., 2012. Relationship between particulate matter and childhood asthma – basis of a future warning system for central Phoenix. Atmos. Chem. Phys. 12. 2479—2490.
- Draxler, R., Stunder, B., Rolph, G., Stein, A., Taylor, A., 2009. HYSPLIT4 User's Guide. El-Gayar, M.S., Abdelfattah, A.E., Barakat, A.O., 2002. Maturity-dependent geochemical markers of crude petroleums from Egypt. Petroleum Sci. Technol. 20. 1057–1070.
- Emeis, S., Schäfer, K., Münkel, C., 2008. Surface-based remote sensing of the mixing-layer height a review. Meteorol. Z. 17, 621—630.
- Fabbri, D., Marynowski, L., Fabianska, M.J., Zaton, M., Simoneit, B.R.T., 2008. Levo-glucosan and other cellulose markers in pyrolysates of Miocene lignites: geochemical and environmental implications. Environ. Sci. Technol. 42, 2957–2963.
- Fabbri, D., Torri, C., Simoneit, B.R.T., Marynowski, L., Rushdi, A.I., Fabiańska, M.J., 2009. Levoglucosan and other cellulose and lignin markers in emissions from burning of Miocene lignites. Atmos. Environ. 43, 2286–2295.
- Fromme, H., Lahrz, T., Hainsch, A., Oddoy, A., Piloty, M., Ruden, H., 2005. Elemental carbon and respirable particulate matter in the indoor air of apartments and nursery schools and ambient air in Berlin (Germany). Indoor Air 15, 335–341.
- Gu, J.W., Pitz, M., Schnelle-Kreis, J., Diemer, J., Reller, A., Zimmermann, R., Soentgen, J., Stoelzel, M., Wichmann, H.E., Peters, A., Cyrys, J., 2011. Source apportionment of ambient particles: comparison of positive matrix factorization analysis applied to particle size distribution and chemical composition data. Atmos. Environ. 45, 1849–1857.
- Gussman, R.A., 1969. On the aerosol particle slip correction factor. J. Appl. Meteorol. 8, 999–1001.
- Han, Y.M., Cao, J.J., Chow, J.C., Watson, J.G., An, Z.S., Liu, S.X., 2009. Elemental carbon in urban soils and road dusts in Xi'an, China and its implication for air pollution. Atmos. Environ. 43, 2464–2470.
- He, L.Y., Hu, M., Huang, X.F., Zhang, Y.H., Tang, X.Y., 2006. Seasonal pollution characteristics of organic compounds in atmospheric fine particles in Beijing. Sci. Total Environ. 359, 167–176.
- Huang, K., Zhuang, G., Lin, Y., Fu, J.S., Wang, Q., Liu, T., Zhang, R., Jiang, Y., Deng, C., Fu, Q., Hsu, N.C., Cao, B., 2012. Typical types and formation mechanisms of haze in an Eastern Asia megacity, Shanghai. Atmos. Chem. Phys. 12, 105–124.
- Huang, X.F., He, L.Y., Hu, M., Zhang, Y.H., 2006. Annual variation of particulate organic compounds in PM2.5 in the urban atmosphere of Beijing. Atmos. Environ. 40, 2449–2458.
- Ianniello, A., Spataro, F., Esposito, G., Allegrini, I., Hu, M., Zhu, T., 2011. Chemical characteristics of inorganic ammonium salts in PM2.5 in the atmosphere of Beijing (China). Atmos. Chem. Phys. 11, 10803–10822.
- IPCC, 2013. In: Stocker, T.F., Qin, D., Plattner, G.K., et al. (Eds.), Climate Change 2013: the Physical Science Basis. Contribution of Working Group I to the Fifth Assessment Report of the Intergovernmental Panel on Climate Change. Cambridge University Press, Cambridge, United Kingdom and New York, NY, USA.
- Ji, D.S., Li, L., Wang, Y.S., Zhang, J.K., Cheng, M.T., Sun, Y., Liu, Z., Wang, L., Tang, G., Hu, B., Chao, N., Wen, T., Miao, H., 2014. The heaviest particulate air-pollution episodes occurred in northern China in January, 2013: Insights gained from observation. Atmos. Environ. 92, 546–556.
- Jung, C.H., Kim, Y.P., 2006. Numerical estimation of the effects of condensation and coagulation on visibility using the moment method. J. Aerosol Sci. 37, 143—161.
- Keil, C., Kassa, H., Brown, A., Kumie, A., Tefera, W., 2010. Inhalation exposures to particulate matter and carbon monoxide during Ethiopian coffee ceremonies in Addis Ababa: a pilot study. J. Environ. Public Health. http://dx.doi.org/10.1155/ 2010/213960. Article ID 213960.
- Kelly, G.M., Taubman, B.F., Perry, L.B., Sherman, J.P., Soulé, P.T., Sheridan, P.J., 2012. Aerosol-precipitation interactions in the southern Appalachian Mountains. Atmos. Chem. Phys. Discuss. 12, 5487–5517.
- Kleeman, M.J., Riddle, S.G., Robert, M.A., Jakober, C.A., Fine, P.M., Hays, M.D., Schauer, J.J., Hannigan, M.P., 2009. Source apportionment of fine (PM1.8) and ultrafine (PM0.1) airborne particulate matter during a severe winter pollution episode. Environ. Sci. Technol. 43, 272–279.
- Kramar, U., 1999. 1999 Methods and Instrumentation X ray Fluorescence Spectrometers. Encyclopedia of Spectroscopy and Spectrometry, pp. 2467–2477.
- Lei, C., Landsberger, S., Basunia, S., Tao, Y., 2004. Study of PM2.5 in Beijing suburban site by neutron activation analysis and source apportionment. J. Radioanalytical Nucl. Chem. 261, 87–94.
- Li, M.M., Huang, X., Zhu, L., Li, J., Song, Y., Cai, X., Xie, S., 2012b. Analysis of the transport pathways and potential sources of PM10 in Shanghai based on three methods. Sci. Total Environ. 414, 525–534.
- Li, X.R., Wang, L.L., Wang, Y.S., Wen, T.X., Yang, Y.J., Zhao, Y.N., Wang, Y.F., 2012a. Chemical composition and size distribution of airborne particulate matters in Beijing during the 2008 Olympics. Atmos. Environ. 50, 278–286.
- Li, Y., Wang, W., Kan, H.D., Xu, X.H., Chen, B.H., 2010. Air quality and outpatient visits for asthma in adults during the 2008 Summer Olympic Games in Beijing. Sci. Total Environ. 408, 1226–1227.

- Marple, V.A., Liu, B.Y.H., 1974. Characteristics of laminar jet impactors. Environ. Sci. Technol. 8, 648–654.
- Marple, V.A., Willeke, K., 1976. Impactor design. Atmos. Environ. 10, 891–896.
- Münkel, C., Eresmaa, N., Rasanen, J., Karppinen, A., 2007. Retrieval of mixing height and dust concentration with lidar ceilometer. Boundary-Layer Meteorol. 124, 117–128
- Niu, H., Shao, L., Zhang, D., 2011. Aged status of soot particles during the passage of a weak cyclone in Beijing. Atmos. Environ. 45, 2699–2703.
- Norris, G., Vedantham, R., Wade, K., Brown, S., Prouty, J., Foley, C., 2008. EPA Positive Matrix Factorization (PMF) 3.0 Fundamentals & User Guide.
- Orasche, J., Schnelle-Kreis, J., Ábbaszade, G., Zimmermann, R., 2011. Technical Note: In-situ derivatization thermal desorption GC-TOFMS for direct analysis of particle-bound non-polar and polar organic species. Atmos. Chem. Phys. 11, 8977–8993.
- Oros, D.R., Simoneit, B.R.T., 2000. Identification and emission rates of molecular tracers in coal smoke particulate matter. Fuel 79, 515–536.
- Paatero, P., 1997. Least squares formulation of robust non-negative factor analysis. Chemom. Intelligent Laboratory Syst. 37, 23–35.
- Paatero, P., Hopke, P.K., 2003. Discarding or downweighting high-noise variables in factor analytic models. Anal. Chim. Acta 490, 277–289.
- Paatero, P., Tapper, U., 1993. Analysis of different modes of factor analysis as least squares fit problems. Chemom. Intell. Lab. Syst. 18, 183–194.
- Paatero, P., Tapper, U., 1994. Positive matrix factorization: a non-negative factor model with optimal utilization of error estimates of data values. Environmetrics 5, 111–126
- Phuleria, H.C., Geller, M.D., Fine, P.M., Sioutas, C., 2006. Size-resolved emissions of organic tracers from light- and heavy-duty vehicles measured in a California roadway tunnel. Environ. Sci. Technol. 40, 4109—4118.
- Polissar, A.V., Hopke, P.K., Paatero, P., Malm, W.C., Sisler, J.F., 1998. Atmospheric aerosol over Alaska: 2. Elemental composition and sources. J. Geophys. Res. Atmos. 103, 19045–19057.
- Rastogi, N., Singh, A., Singh, D., Sarin, M.M., 2014. Chemical characteristics of PM2.5 at a source region of biomass burning emissions: evidence for secondary aerosol formation. Environ. Pollut. 184, 563–569.
- Reff, A., Eberly, S.I., Bhave, P.V., 2007. Receptor modeling of ambient particulate matter data using positive matrix factorization: review of existing methods. J. Air & Waste Manag. Assoc. 57, 146—154.
- Rogge, W.F., Hildemann, L.M., Mazurek, M.A., Cass, G.R., Simoneit, B.R.T., 1993. Sources of fine organic aerosol. 2. Noncatalyst and catalyst-equipped automobiles and heavy-duty diesel trucks. Environ. Sci. Technol. 27, 636–651.
- Schäfer, K., Elsasser, M., Arteaga-Salas, J.M., Gu, J., Pitz, M., Schnelle-Kreis, J., Cyrys, J., Emeis, S., Prevot, A.S.H., Zimmermann, R., 2014. Source apportionment and the role of meteorological conditions in the assessment of air pollution exposure due to urban emissions. Atmos. Chem. Phys. Discuss. 14, 2235–2275.
- Schäfer, K., Emeis, S., Hoffmann, H., Jahn, C., 2006. Influence of mixing layer height upon air pollution in urban and sub-urban areas. Meteorol. Z. 15, 647–658.
- Schäfer, K., Emeis, S., Schrader, S., Török, S., Alföldy, B., Osan, J., Pitz, M., Münkel, C., Cyrys, J., Peters, A., Sarigiannis, D., Suppan, P., 2011. A measurement based analysis of the spatial distribution, temporal variation and chemical composition of particulate matter in Munich and Augsburg. Meteorol. Z. 20, 47–57.
- Schnelle-Kreis, J., Sklorz, M., Orasche, J., Stolzel, M., Peters, A., Zimmermann, R., 2007. Semi volatile organic compounds in ambient PM2.5. Seasonal trends and daily resolved source contributions. Environ. Sci. Technol. 41, 3821–3828.
- Seinfeld, J.H., Pandis, S.N., 2006. Atmospheric Chemistry and Physics: from Air Pollution to Climate Change, second ed. John Wiley & Sons Inc, New Jersey, U.S.
- Shao, L.Y., Li, J.J., Zhao, H.Y., Yang, S.S., Li, H., Li, W.J., Jones, T., Sexton, K., BéruBé, K., 2007. Associations between particle physicochemical characteristics and oxidative capacity: an indoor PM10 study in Beijing, China. Atmos. Environ. 41, 5316–5326.
- Shao, L.Y., Shi, Z.B., Jones, T.P., Li, J.J., Whittaker, A.G., BéruBé, K.A., 2006. Bioreactivity of particulate matter in Beijing air: results from plasmid DNA assay. Sci. Total Environ. 367, 261–272.
- Shi, G., Chen, Z., Bi, C., Li, Y., Teng, J., Wang, L., Xu, S., 2010. Comprehensive assessment of toxic metals in urban and suburban street deposited sediments (SDSs) in the biggest metropolitan area of China. Environ. Pollut. 158, 694–703.
- Shi, Z.B., Shao, L.Y., Jones, T.P., Lu, S.L., 2005. Microscopy and mineralogy of airborne particles collected during severe dust storm episodes in Beijing, China. J. Geophys. Res. Atmos. 110, D01303.
- Song, S.J., Wu, Y., Jiang, J.K., Yang, L., Cheng, Y., Hao, J.M., 2012. Chemical characteristics of size-resolved PM2.5 at a roadside environment in Beijing, China. Environ. Pollut. 161, 215–221.
- Song, Y., Tang, X.Y., Xie, S.D., Zhang, Y.H., Wei, Y.J., Zhang, M.S., Zeng, L.M., Lu, S.H., 2007. Source apportionment of PM2.5 in Beijing in 2004. J. Hazard. Mater. 146, 124–130.
- Song, Y., Zhang, Y.H., Xie, S.D., Zeng, L.M., Zheng, M., Salmon, L.G., Shao, M., Slanina, S., 2006. Source apportionment of PM2.5 in Beijing by positive matrix factorization. Atmos. Environ. 40, 1526–1537.
- Soriano, A., Pallarés, S., Pardo, F., Vicente, A.B., Sanfeliu, T., Bech, J., 2012. Deposition of heavy metals from particulate settleable matter in soils of an industrialised area. J. Geochem. Explor. 113, 36–44.
- Sun, Y.L., Wang, Z.F., Dong, H.B., Yang, T., Li, J., Pan, X.L., Chen, P., Jayne, J.T., 2012. Characterization of summer organic and inorganic aerosols in Beijing, China with an aerosol chemical speciation monitor. Atmos. Environ. 51, 250–259.

- Tian, H., Wang, Y., Xue, Z., Cheng, K., Qu, Y., Chai, F., Hao, J., 2010. Trend and characteristics of atmospheric emissions of Hg, As, and Se from coal combustion in China, 1980–2007. Atmos. Chem. Phys. 10, 11905–11919.
- Turpin, B.J., Lim, H.J., 2001. Species contributions to PM2.5 mass concentrations: revisiting common assumptions for estimating organic mass. Aerosol Sci. Technol. 35, 602–610.
- Wagener, S., Langner, M., Hansen, U., Moriske, H.-J., Endlicher, W.R., 2012. Spatial and seasonal variations of biogenic tracer compounds in ambient PM10 and PM1 samples in Berlin, Germany. Atmos. Environ. 47, 33–42.
- Wang, H., Zhuang, Y., Wang, Y., Sun, Y., Yuan, H., Zhuang, G., Hao, Z., 2008. Long-term monitoring and source apportionment of PM2.5/PM10 in Beijing, China. J. Environ. Sci. 20, 1323–1327.
- Wang, H.L., Zhou, Y.M., Zhuang, Y.H., Wang, X.K., Hao, Z.P., 2009. Characterization of PM2.5/PM2.5—10 and source tracking in the juncture belt between urban and rural areas of Beijing, Chin. Sci. Bull. 54, 2506—2515.
- Wang, S.L., Mulligan, C.N., 2006. Occurrence of arsenic contamination in Canada: sources, behavior and distribution. Sci. Total Environ. 366, 701–721. Wang, Y.S., Ren, X.Y., Ji, D.S., Zhang, J.Q., Sun, J., Wu, F.K., 2012. Characterization of
- Wang, Y.S., Ren, X.Y., Ji, D.S., Zhang, J.Q., Sun, J., Wu, F.K., 2012. Characterization of volatile organic compounds in the urban area of Beijing from 2000 to 2007. J. Environ. Sci. 24, 95–101.
- Wu, Y., Yang, L., Zheng, X., Zhang, S.J., Song, S.J., Li, J.Q., Hao, J.M., 2014. Characterization and source apportionment of particulate PAHs in the roadside environment in Beijing, Sci. Total Environ. 470–471, 76–83.
- Xin, J.Y., Zhang, Q., Wang, L.L., Gong, C.S., Wang, Y.S., Liu, Z.R., Gao, W.K., 2014. The empirical relationship between the PM2.5 concentration and aerosol optical depth over the background of North China from 2009 to 2011. Atmos. Res. 138, 179–188.
- Xu, L.L., Chen, X.Q., Chen, J.S., Zhang, F.W., He, C., Zhao, J.P., Yin, L.Q., 2012. Seasonal variations and chemical compositions of PM2.5 aerosol in the urban area of Fuzhou, China. Atmos. Res. 104–105, 264–272.
- Yang, F., Huang, L., Duan, F., Zhang, W., He, K., Ma, Y., Brook, J.R., Tan, J., Zhao, Q., Cheng, Y., 2011. Carbonaceous species in PM2.5 at a pair of rural/urban sites in Beijing, 2005–2008. Atmos. Chem. Phys. 11, 7893–7903.

- Yang, F.M., Ye, B.M., He, K.B., Ma, Y.L., Cadle, S.H., Chan, T., Mulawa, P.A., 2005. Characterization of atmospheric mineral components of PM2.5 in Beijing and Shanghai, China. Sci. Total Environ. 343, 221–230.
- Yang, G.S., Ma, L.L., Xu, D.D., Li, J., He, T.T., Liu, L.Y., Jia, H.L., Zhang, Y.B., Chen, Y., Chai, Z.F., 2012. Levels and speciation of arsenic in the atmosphere in Beijing, China. Chemosphere 87, 845–850.
- Yao, X.H., Chan, C.K., Fang, M., Cadle, S., Chan, T., Mulawa, P., He, K.B., Ye, B.M., 2002. The water-soluble ionic composition of PM2.5 in Shanghai and Beijing, China. Atmos. Environ. 36, 4223—4234.
- Yu, L.D., Wang, G.F., Zhang, R.J., Zhang, L.M., Song, Y., Wu, B.B., Li, X.F., An, K., Chu, J.H., 2013. Characterization and source apportionment of PM2.5 in an urban environment in Beijing. Aerosol Air Qual. Res. 13, 574–583.
- Zhang, R.J., Han, Z.W., Cheng, T.T., Tao, J., 2009b. Chemical properties and origin of dust aerosols in Beijing during springtime. Particuology 7, 61–67.
- Zhang, T., Claeys, M., Cachier, H., Dong, S.P., Wang, W., Maenhaut, W., Liu, X.D., 2008. Identification and estimation of the biomass burning contribution to Beijing aerosol using levoglucosan as a molecular marker. Atmos. Environ. 42, 7013–7021.
- Zhang, W., Guo, J.H., Sun, Y.L., Yuan, H., Zhuang, G.S., Zhuang, Y.H., Hao, Z.P., 2007. Source apportionment for urban PM10 and PM2.5 in the Beijing area. Chin. Sci. Bull. 52. 608—615.
- Zhang, Y., Sheesley, R.J., Bae, M.-S., Schauer, J.J., 2009a. Sensitivity of a molecular marker based positive matrix factorization model to the number of receptor observations. Atmos. Environ. 43, 4951–4958.
- Zhao, P.S., Dong, F., He, D., Zhao, X.J., Zhang, X.L., Zhang, W.Z., Yao, Q., Liu, H.Y., 2013b. Characteristics of concentrations and chemical compositions for PM2.5 in the region of Beijing, Tianjin, and Hebei, China. Atmos. Chem. Phys. 13, 4631–4644
- Zhao, P.S., Dong, F., Yang, Y.D., He, D., Zhao, X.J., Zhang, W.Z., Yao, Q., Liu, H.Y., 2013a. Characteristics of carbonaceous aerosol in the region of Beijing, Tianjin, and Hebei, China. Atmos. Environ. 71, 389—398.
- Zhu, L., Huang, X., Shi, H., Cai, X., Song, Y., 2011. Transport pathways and potential sources of PM10 in Beijing. Atmos. Environ. 45, 594–604.